Remote sensing of sea-ice thickness in the Weddell Sea

Calvin T. Swift, Karen M. St. Germain, *and* James D. Menashi

Microwave Remote Sensing Laboratory
University of Massachusetts
Boston, Massachusets 02116

As part of the Winter Weddell Gyre Experiment 1989, we investigated the feasibility of remotely measuring antarctic sea-ice thickness using passive microwave techniques. A description of our field operations, which involved measuring the brightness temperature of sea ice in the Weddell Sea at 611 megahertz, appeared in the 1990 *Antarctic Journal of the U.S.* review issue (St. Germain and Swift 1990). The data have now been analyzed and correlated with *in situ* thickness measurements, video recordings, and other passive microwave data. The results of this study indicate that ice thickness can be measured reliably up to 75 centimeters with the 611-megahertz radiometer.

Our study is based on the concept that all materials constantly emit electromagnetic energy. The intensity of this radiation depends on the dielectric and physical properties of the material. A microwave radiometer measures the power level of incoming radiation. This power level is commonly expressed as a *brightness temperature* based on the following relationship:

$$P = k \times T_b \times B \Rightarrow T_b = P \div (k \times B) \qquad \text{(equation 1)}$$

where

P = power of received radiation
T_b = brightness temperature
k = Boltzman's constant
B = bandwidth of the instrument

For a flat surface, the brightness temperature is proportional to physical temperature of the surface as:

$$T_b = e \times T = (1 - r) \times T \qquad \text{(equation 2)}$$

where

e = emissivity
r = Fresnel reflection coefficient

For layered media such as sea ice, the brightness temperature measured is a composite, in this case, of the ice and the underlying water. Experience with C-Band (4–8 gigahertz) passive sea-ice measurements suggests that under usual growth conditions the apparent brightness temperature of an ice layer increases monotonically from the low, open-water value to the relatively high, thick-ice value. The upper limit of the brightness temperature occurs when the ice reaches roughly 1½ free-space wavelengths in thickness (70 centimeters for 611 megahertz, 5 centimeters for 10 gigahertz). This behavior suggests that it should be possible to measure ice thickness via brightness temperature. Swift et al. (1986) developed a theoretical model based on work done by Apinis and Peak (1976) which describes the emissivity as a function of ice thickness. This, combined with equation 2, provides the necessary relationship between the measurable brightness temperature and the desired product, ice thickness.

The field measurements were made using a ultra-high-frequency (611 megahertz) radiometer that was mounted on the port side of the *Polarstern*, looking downward to the ice at an angle of 35° off nadir. A 10-gigahertz radiometer was mounted on the rail next to the ultra-high-frequency radiometer, operating at a 53° incidence angle. Adjacent to the radiometers, a handheld video camera was operated while the ship traveled through the ice, providing a record of ice coverage within the footprint, ice thickness, and details such as ridges and hummocks. Whenever possible, several field groups on board made extensive *in situ* measurements of thickness distribution and snow-cover characteristics, similar to previously documented work (Wadhams, Lange, and Ackley 1987; Wadhams 1988).

An algorithm was developed to reduce the raw brightness temperature data to ice thickness estimates, taking into account variables such as background noise and physical temperature. A curve illustrating the model relationship between brightness temperature and ice thickness, assuming typical values of tem-

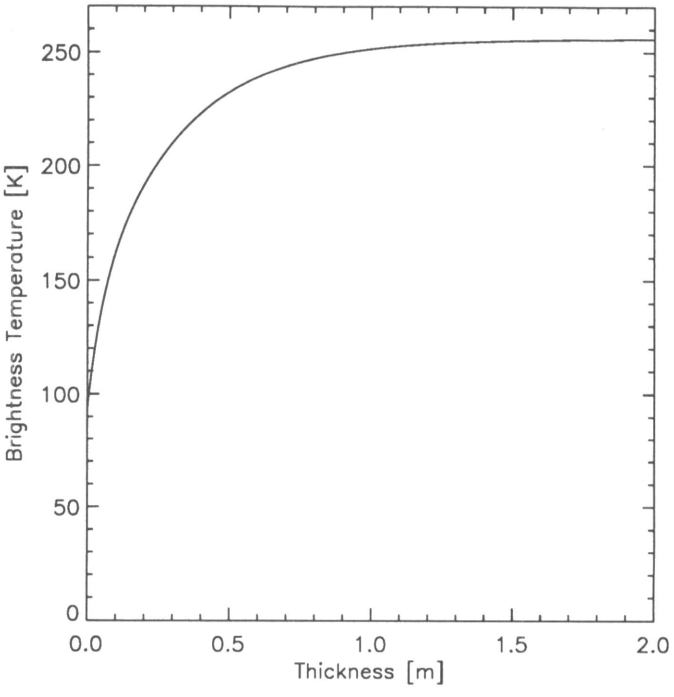

Figure 1. Model relationship between brightness temperature and ice thickness at 611 megahertz for typical values of temperature and dielectric constant. (Tb denotes brightness temperature. K denotes kelvin. m denotes meter.)

perature and dielectric constant, is shown in figure 1. Ice thickness estimates based on this relationship were then compared with the video, *in situ*, and 10-gighertz data. As an example, consider the time series of figure 2, where we have plotted the brightness temperatures of consolidated antarctic sea ice collected at 10 gigahertz (upper trace) and at ultra-high frequency (lower trace). These data were collected along an ice floe where ice corings and videotape were available for comparison. Note that the 10-gigahertz signal is flat until the edge of the floe is encountered, at which point the brightness temperature approaches that of open water. On the other hand, the ultra-high-frequency signature varies throughout the transect of the ship, which we attribute to changes in the ice thickness.

The ice thickness estimates derived from the ultra-high-frequency data are shown in figure 3. The sharp peak in thickness at 7 minutes on the time axis is an observable maximum in thickness, and ice cores from the same floe indicated thicknesses ranging from 0.6 to 1.0 meters with a hard snow cover. The minima at 2 and 9.5 minutes correspond to an area of gray-white ice which, although its thickness could not safely be measured *in situ*, can be estimated to be 20–30 centimeters thick.

Other time-series data sets occasionally showed a correlation between the 10-gigahertz data and the ultra-high-frequency data. There are two situations for which this is expected. In the case of very thin ice (less than 5 centimeter thick), both radiometers respond to thickness, and thus exhibit similar behavior. For thick ice, however, a correlation between the high- and low-frequency data indicates fluctuations in surface and dielectric characteristics. These results suggest that a higher frequency microwave radiometer should be used in conjunction with a ultra-high-frequency radiometer to correct thickness estimates for variations introduced by surface phenomena. Additional data have been reduced, and will be included in a technical paper.

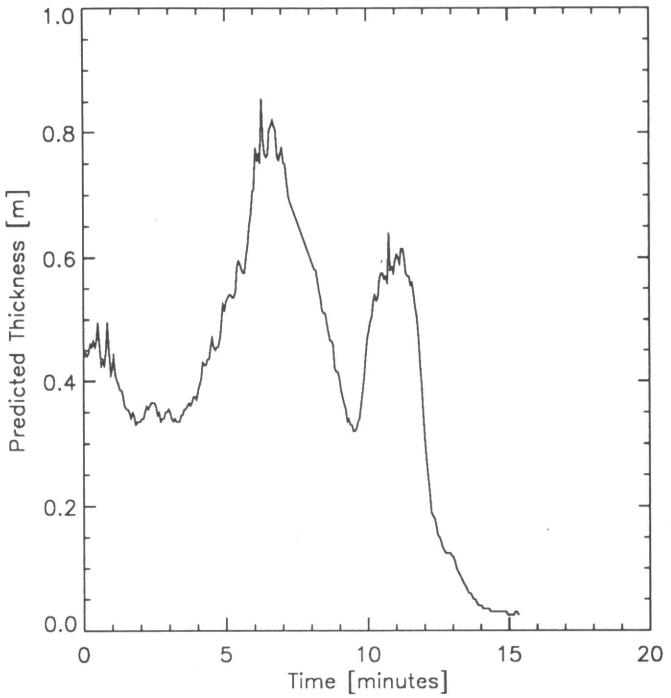

Figure 3. Estimated ice thickness based on the ultra-high-frequency data shown in figure 2 and the model curve given in figure 1. (m denotes meter.)

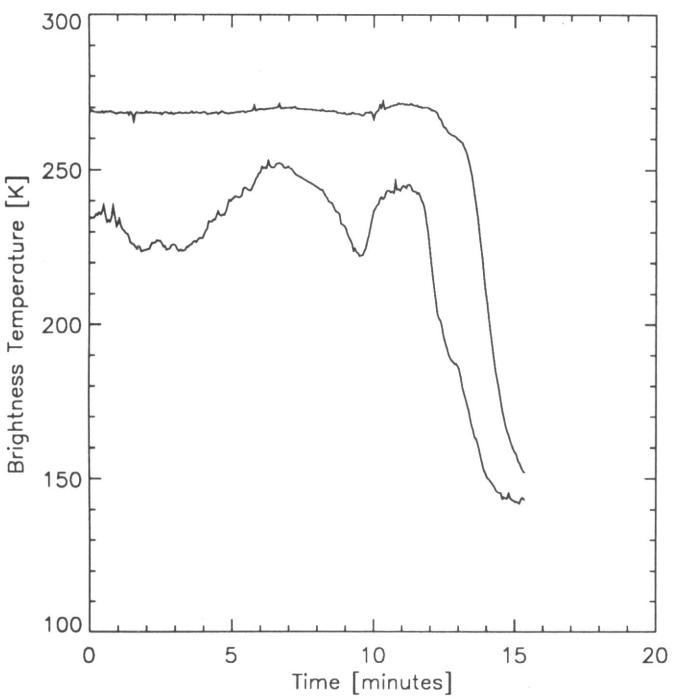

Figure 2. Brightness temperature time series at ultra high frequency (lower trace) and 10-gigahertz frequency (upper trace) as the ship moved along a floe. (Tb denotes brightness temperature. K denotes kelvin. UHF denotes ultra high frequency. GHz denotes gigahertz.)

References

Apinis, J.J., and W.H. Peak. 1976. *Passive microwave mapping of ice thickness.* ElectroScience Report 3892-2, August 1976. Columbus: Ohio State University.

St. Germain, K., and C.T. Swift. 1990. Brightness temperature measurements, at 611 megahertz, of sea ice in the Weddell Sea. *Antarctic Journal of the U.S.*, 25(5), 119–120.

Swift, C.T., D.C. D. Hority, A.B. Tanner, and R.E. McIntosh. 1986. Passive microwave spectral emission from saline ice at C-band during growth phase. *IEEE Transactions, Geology and Remote Sensing*, GE-24, 840–848.

Wadhams, P. 1988. The underside of arctic sea ice imaged by sidescan sonar. *Nature*, 333, 161–164.

Wadhams, P., M.A. Lange, and S.F. Ackley. 1987. The ice thickness distribution across the Atlantic sector of the antarctic ocean in midwinter. *Journal of Geophysical Research*, 92 (C13), 14,535–14,552.